

Fast global spectral methods for three-dimensional partial differential equations

Christoph Strössner¹ and Daniel Kressner²

¹Institute of Mathematics, EPF Lausanne, Switzerland, christoph.stroessner@epfl.ch.

²Institute of Mathematics, EPF Lausanne, Switzerland, daniel.kressner@epfl.ch.

November 9, 2021

Abstract

Global spectral methods offer the potential to compute solutions of partial differential equations numerically to very high accuracy. In this work, we develop a novel global spectral method for linear partial differential equations on cubes by extending ideas of Chebop2 [Townsend and Olver, *J. Comput. Phys.*, 299 (2015)] to the three-dimensional setting utilizing expansions in tensorized polynomial bases. Solving the discretized PDE involves a linear system that can be recast as a linear tensor equation. Under suitable additional assumptions, the structure of these equations admits for an efficient solution via the blocked recursive solver [Chen and Kressner, *Numer. Algorithms*, 84 (2020)]. In the general case, when these assumptions are not satisfied, this solver is used as a preconditioner to speed up computations.

1 Introduction

This work is concerned with the solution of linear partial differential equations (PDEs) on cubes using global spectral methods [20, 26, 57, 59]. The solution is approximated globally on the whole domain in terms of a truncated (tensorized) Chebyshev series [67, 42, 60]. For one- and two-dimensional rectangular domains this approach led to the development of the solvers Chebop [16, 46, 17] and Chebop2 [57] contained in the Chebfun package [18] for computing numerically with functions. Many models used in medicine [32, 39, 54], engineering [5, 19, 50] and geosciences [33, 43, 68] involve PDEs on three-dimensional domains. These domains are rarely cubes, but they can often be embedded in or mapped onto cubes. Whilst the efficient approximation of trivariate functions on cubes by combining tensorized Chebyshev interpolation and low-rank approximations has been studied in Chebfun3 [30] and Chebfun3F [15], there is no generalization of Chebop2 for three-dimensional PDEs on cubes. So far, the ideas of Chebop2 have been extended to triangular domains [47] and to disks [64, 45]. For the special case of the Poisson equation with homogeneous Dirichlet boundary conditions, extensions to three-dimensional spheres [58], cylinders and unit cubes [22] have been developed.

Throughout this work, we study linear PDEs of the form

$$\mathcal{L}u = f \quad \text{on } [-1, 1]^3, \tag{1}$$

complemented with linear boundary conditions. We approximate u and f in terms of truncated expansions with tensorised polynomial basis functions. These expansions are represented by coefficient tensors of order 3. Global spectral methods approximate the operator \mathcal{L} by a mapping mimicing the impact of applying \mathcal{L} on the level of the coefficient tensors. We compute such a mapping by expressing the the three-dimensional differential operator as combination of one-dimensional linear differential operators, which we determine using a CP decomposition [36]. By representing u in a Chebyshev basis and f in an ultraspherical basis,

we can express the action of these one-dimensional operators on the coefficients in terms of sparse and well-conditioned differentiation and multiplication matrices [46]. The combination of applying these matrices yields the desired mapping. Solving the PDE corresponds to inverting this mapping, which can be seen as solving a tensor-valued linear system. Discretizing the boundary conditions provides additional linear constraints under which inverting the linear system has a unique solution. Using substitution we obtain an unconstrained tensor-valued linear system uniquely determining a subtensor, from which we recover the full coefficient tensor of the solution.

It turns out that our discretization of the PDE (1) has Kronecker structure, which can often be exploited. For instance, Poisson’s equation with homogeneous Dirichlet boundary conditions leads to a Laplace-like equation [4, 10, 37, 44]. Laplace-like equations can be solved efficiently using the blocked recursive algorithm in cite [9]. This algorithm is asymptotically slower than the nested alternating direction implicit method in [22], but our numerical experiments in Section 5 demonstrate that the recursive blocked algorithm is significantly faster in practice. Even if the PDE of interest does not immediately lead to a structure suitable for the fast solver, we can often still apply the blocked recursive algorithm as preconditioner for GMRES.

The algorithmic ideas presented in this work, can not only be applied to from solving stationary linear PDEs, such as the Helmholtz equation and (convection) diffusion problems. We present further extensions to time-dependent PDEs and PDE eigenvalue problems of the form

$$\frac{\partial}{\partial t}u = \mathcal{L}u \quad \text{and} \quad \mathcal{L}u = \lambda u,$$

which we solve using implicit Euler and inverse iteration methods respectively.

The global spectral method can be used to compute solutions numerically to very high accuracy. It is not to be confused with so called spectral element methods [21, 31, 34] and p - and hp -finite element methods [2, 45, 66], where u is represented as sum of individual elements, each of which are approximated using truncated series expansions, instead of a global approximation of u . There also exist solvers relying on using domain decompositions in combination with truncated series expansions [28, 48]. We want to emphasize that the methods presented in this work can be used as local solver, when the elements/subdomains can be mapped to cubes.

The remainder of this paper is structured as follows. In Section 2, we define linear differential operators and the approximation format. In Section 3, we derive the mapping on the level of the coefficient tensor for linear differential operators. The discretization of PDEs and the efficient solution of the resulting tensor-valued linear system is discussed in Section 4. In Section 5, we apply our global spectral method to solve stationary PDEs, parabolic PDEs and PDE eigenvalue problems numerically to very high accuracy.

2 Problem setting

2.1 Structure of a linear differential operator

A linear partial differential operator \mathcal{L} on the domain $[-1, 1] \times [-1, 1] \times [-1, 1]$ maps a sufficiently smooth function $u : [-1, 1]^3 \rightarrow \mathbb{R}$ to

$$\mathcal{L}u(x, y, z) = \sum_{a=0}^{N_x} \sum_{b=0}^{N_y} \sum_{c=0}^{N_z} \alpha_{abc}(x, y, z) \frac{\partial^{a+b+c}}{\partial x^a \partial y^b \partial z^c} u(x, y, z), \tag{2}$$

where N_x, N_y, N_z are called differential order and $\alpha_{abc}(x, y, z) : [-1, 1]^3 \rightarrow \mathbb{R}$ are coefficient functions for $1 \leq a \leq N_x, 1 \leq b \leq N_y, 1 \leq c \leq N_z$. For the differential operator \mathcal{L} we consider the linear PDE

$$\mathcal{L}u = f \tag{3}$$

with right hand side $f(x, y, z) : [-1, 1]^3 \rightarrow \mathbb{R}$. The PDE can be solved uniquely when the system is complemented with sufficient boundary conditions.

2.2 Approximation format

We approximate the solution $u : [-1, 1]^3 \rightarrow \mathbb{R}$ of the PDE (3) in the space $\mathbb{P}_{n_1, n_2, n_3}$ of trivariate polynomials of degree at most (n_1, n_2, n_3) . We express u in terms of a tensorised basis of Chebyshev polynomials, which leads to a representation of the form

$$u(x, y, z) \approx \sum_{i=1}^{n_1} \sum_{j=1}^{n_2} \sum_{k=1}^{n_3} \mathcal{U}_{ijk} T_i(x) T_j(y) T_k(z), \quad (4)$$

where $\mathcal{U} \in \mathbb{R}^{n_1 \times n_2 \times n_3}$ is called coefficient tensor and $T_k(x) = \cos((k-1) \cos^{-1}(x))$ denotes the k -th Chebyshev polynomial.

3 Operator discretization

In the following, we discretize the differential operator \mathcal{L} by approximating \mathcal{L} as mapping from $\mathbb{P}_{n_1, n_2, n_3}$ to $\mathbb{P}_{n_1, n_2, n_3}$. This is particularly easy for constant coefficients in the differential operator \mathcal{L} , i.e. $\alpha_{abc}(x, y, z) = \alpha_{abc} \in \mathbb{R}$ in Equation (2). Applying a linear differential operator with constant coefficients to a polynomial does not increase the polynomial degree. For non-constant coefficients an additional truncation is need to obtain a polynomial in $\mathbb{P}_{n_1, n_2, n_3}$. Thus, it is natural to see the application of the operator as a change of the coefficient tensor. We discuss the discretization for the constant case first before generalizing to the non-constant case in Section 3.3.

3.1 One-dimensional differential operators

We briefly recapitulate how to obtain the mapping describing the change of coefficients in a one-dimensional setting before returning to the three-dimensional setting. Let $u : [-1, 1] \rightarrow \mathbb{R}$ be a polynomial of degree n represented in Chebyshev basis by $u(x) = \sum_{k=1}^n u_k T_k(x)$, with coefficients $u_k \in \mathbb{R}$ and Chebyshev polynomials $T_k(x)$. Applying a one-dimensional linear differential operator \mathcal{L} with constant coefficients to u can be written as

$$\mathcal{L}u(x) = \sum_{a=0}^N \alpha_a \frac{d^a}{dx^a} u(x), \quad (5)$$

with coefficients $\alpha_a \in \mathbb{R}$. This is a linear combination of (higher order) derivatives of u . For every derivative of the polynomial u , there exist so a called differentiation matrix which maps the coefficient vector $\mathbf{u} = (u_1, \dots, u_n)$ to the coefficients of the derivative. The remainder of this section follows the ideas of [46] to represent the derivative using an ultraspherical basis instead of a Chebyshev basis, which leads to better conditioned and sparse differentiaton matrices.

For the parameter $\lambda \in \mathbb{N}$ and $k = 3, 4, \dots$, ultraspherical polynomials follow the recurrence relation

$$C_{k+2}^{(\lambda)}(x) = \frac{2(k+\lambda)}{k+1} x C_{k+1}^{(\lambda)}(x) - \frac{k+2\lambda-1}{k+1} C_k^{(\lambda)}(x),$$

which is initialized using $C_1^{(\lambda)}(x) = 1$, $C_2^{(\lambda)}(x) = 2\lambda x$. Let $v(x) = \sum_{k=1}^n v_k C_k^{(\lambda)}(x)$ denote the λ th derivative of u represented in $C^{(\lambda)}$ basis, then the coefficient vector $\mathbf{v} = (v_1, \dots, v_n)$ satisfies $\mathbf{v} = D_\lambda \mathbf{u}$, where the

sparse differentiation matrix $D_\lambda \in \mathbb{R}^{n \times n}$ is defined as

$$D_\lambda = 2^{\lambda-1}(\lambda-1)! \begin{pmatrix} \overbrace{0 \dots 0}^{\lambda \text{ times}} & \lambda & & & & & & & \\ & \lambda+1 & & & & & & & \\ & & \ddots & & & & & & \\ & & & \ddots & & & & & \\ & & & & n-\lambda & & & & \\ & & & & 0 & & & & \\ & & & & \vdots & & & & \\ & & & & 0 & & & & \end{pmatrix}.$$

Note that the ultraspherical basis is different for different λ . The sparse transformation matrices $S_0 \in \mathbb{R}^{n \times n}$, mapping Chebyshev to $C^{(1)}$ coefficients, and $S_\lambda \in \mathbb{R}^{n \times n}$, mapping $C^{(\lambda)}$ to $C^{(\lambda+1)}$, are defined as

$$S_0 = \begin{pmatrix} 1 & 0 & -\frac{1}{2} & & & & & & \\ & \frac{1}{2} & 0 & -\frac{1}{2} & & & & & \\ & & \frac{1}{2} & 0 & -\frac{1}{2} & & & & \\ & & & \ddots & & \ddots & & & \\ & & & & & & \ddots & & \end{pmatrix}, \quad S_\lambda = \begin{pmatrix} 1 & 0 & -\frac{\lambda}{\lambda+2} & & & & & & \\ & \frac{\lambda}{\lambda+1} & 0 & -\frac{\lambda}{\lambda+3} & & & & & \\ & & \frac{\lambda}{\lambda+2} & 0 & -\frac{\lambda}{\lambda+4} & & & & \\ & & & \ddots & & \ddots & & & \\ & & & & & & \ddots & & \end{pmatrix}.$$

Let $\mathcal{L}u(x) = \sum_{k=1}^n w_k C_k^{(N)}(x)$ be represented in $C^{(N)}$ ultraspherical basis with coefficient vector $\mathbf{w} = (w_1, \dots, w_n)$, then

$$\mathbf{w} = \underbrace{(a_N D_N + a_{N-1} S_{N-1} D_{N-1} + \dots + a_1 S_{N-1} \dots S_1 D_1 + a_0 S_{N-1} \dots S_0)}_{=L} \mathbf{u}. \quad (6)$$

The matrix $L \in \mathbb{R}^{n \times n}$ describes how the one-dimensional differential operator \mathcal{L} acts on the level of coefficients.

3.2 Three-dimensional differential operators

In Chebop2 [57] it is suggested to split two-dimensional differential operators via an SVD into a sum of one-dimensional operators, for which the matrices L can be computed as in Section 3.1. Such splittings can be generalized to the three-dimensional setting using a CP decomposition.

Let $\mathcal{A} \in \mathbb{R}^{(N_x+1) \times (N_y+1) \times (N_z+1)}$ denote the tensor with entries $\mathcal{A}_{a+1, b+1, c+1}$ given by the coefficients α_{abc} in Equation (2) for $0 \leq a \leq N_x$, $0 \leq b \leq N_y$, $0 \leq c \leq N_z$. A CP decomposition [36] of \mathcal{A} takes the form

$$\mathcal{A} = \sum_{r=1}^R \mathbf{a}^{(r)} \circ \mathbf{b}^{(r)} \circ \mathbf{c}^{(r)}$$

where R is called tensor-rank, \circ denotes the outer product and $\mathbf{a}^{(r)} \in \mathbb{R}^{N_x+1}$, $\mathbf{b}^{(r)} \in \mathbb{R}^{N_y+1}$, $\mathbf{c}^{(r)} \in \mathbb{R}^{N_z+1}$ for $r = 1, \dots, R$.

We can now rewrite the application of \mathcal{L} to u as

$$\mathcal{L}u(x) = \sum_{r=1}^R \underbrace{\sum_{a=0}^{N_x} \mathbf{a}_{a-1}^{(r)} \frac{\partial^a}{\partial x^a}}_{=\mathcal{L}_r^{(x)}} \underbrace{\sum_{b=0}^{N_y} \mathbf{b}_{b-1}^{(r)} \frac{\partial^b}{\partial y^b}}_{=\mathcal{L}_r^{(y)}} \underbrace{\sum_{c=0}^{N_z} \mathbf{c}_{c-1}^{(r)} \frac{\partial^c}{\partial z^c}}_{=\mathcal{L}_r^{(z)}} u(x, y, z), \quad (7)$$

in terms of one-dimensional differential operators $\mathcal{L}_r^{(x)}$, $\mathcal{L}_r^{(y)}$, $\mathcal{L}_r^{(z)}$.

Let $L_r^{(x)} \in \mathbb{R}^{n_1 \times n_1}$, $L_r^{(y)} \in \mathbb{R}^{n_2 \times n_2}$, $L_r^{(z)} \in \mathbb{R}^{n_3 \times n_3}$ denote the matrices L associated with the operators $\mathcal{L}_r^{(x)}, \mathcal{L}_r^{(y)}, \mathcal{L}_r^{(z)}$ as defined in Equation (6). Let u be a polynomial with coefficient tensor $\mathcal{U} \in \mathbb{R}^{n_1 \times n_2 \times n_3}$ satisfying Equation (4) with equality. Then

$$\mathcal{L}u(x, y, z) = \sum_{i=1}^{n_1} \sum_{j=1}^{n_2} \sum_{k=1}^{n_3} \mathcal{V}_{ijk} C_i^{(N_x)}(x) C_j^{(N_y)}(y) C_k^{(N_z)}(z),$$

with coefficient tensor

$$\mathcal{V} = \sum_{r=1}^R \mathcal{U} \times_1 L_r^{(x)} \times_2 L_r^{(y)} \times_3 L_r^{(z)}, \quad (8)$$

where $\mathcal{V} \times_\ell M$ denotes the mode- ℓ multiplication. For a tensor $\mathcal{V} \in \mathbb{R}^{n_1 \times n_2 \times n_3}$ and a matrix $M \in \mathbb{R}^{m \times n_\ell}$ it is defined as the multiplication of every mode- ℓ fiber of \mathcal{V} with M , i.e.

$$(\mathcal{V} \times_\ell M)^{\{\ell\}} = M \mathcal{T}^{\{\ell\}},$$

where $\mathcal{T}^{\{\ell\}}$ denotes the mode- ℓ matricization, which is the matrix containing all mode- ℓ fibers of \mathcal{V} [36].

3.3 Generalization to non-constant coefficients

3.3.1 One-dimensional differential operators

We now consider the one-dimensional differential operator (5) with non-constant coefficients $\alpha_a : [-1, 1] \rightarrow \mathbb{R}$. In this section, we define multiplication matrices to incorporate these coefficients in the discretization.

Let $u(x)$ be a polynomial of the form $u(x) = \sum_{k=1}^n u_k B_k(x)$, with basis functions $B_k(x)$ chosen as Chebyshev polynomials T_k or ultraspherical polynomials $C_k^{(\lambda)}$. To multiply $u(x)$ with a function $v(x) : [-1, 1] \rightarrow \mathbb{R}$, we approximate $v(x) \approx \tilde{v}(x) = \sum_{k=1}^n v_k B_k(x)$ by a polynomial in the same basis using Chebyshev interpolation [60] (and basis transformations). Further, we also approximate the product $\tilde{v}(x)u(x) \approx z(x) = \sum_{k=1}^n z_k B_k(x)$ by a polynomial in the same basis. There exist so called multiplication matrices [46, 21] depending on the coefficients $\mathbf{v} = (v_1, \dots, v_n)$, which map the coefficients $\mathbf{u} = (u_1, \dots, u_n)$ to the coefficients $\mathbf{z} = (z_1, \dots, z_n)$ such that $z(x)$ approximates $v(x)u(x)$ accurately for sufficiently large n . In the following, we summarize how these matrices are defined in [56] for both Chebyshev and ultraspherical bases. For the Chebyshev basis, we define $\mathbf{z} = M[\mathbf{v}]\mathbf{u}$ and the multiplication matrix $M[\mathbf{v}] \in \mathbb{R}^{n \times n}$ given by

$$M[\mathbf{v}] = \frac{1}{2} \begin{pmatrix} 2v_1 & v_2 & v_3 & \dots \\ v_2 & 2v_1 & v_2 & \dots \\ v_3 & v_2 & 2v_1 & \dots \\ \vdots & \vdots & \vdots & \ddots \end{pmatrix} + \frac{1}{2} \begin{pmatrix} 0 & 0 & 0 & \dots \\ v_2 & v_3 & v_4 & \dots \\ v_3 & v_4 & v_5 & \dots \\ \vdots & \vdots & \vdots & \ddots \end{pmatrix}.$$

For the $C^{(\lambda)}$ ultraspherical basis, we define $\mathbf{z} = M^{(\lambda)}[\mathbf{v}]\mathbf{u}$ and the multiplication matrix $M^{(\lambda)}[\mathbf{v}] \in \mathbb{R}^{n \times n}$ as $M^{(\lambda)}[\mathbf{v}] = \sum_{i=1}^n v_i M_i^{(\lambda)}$. The matrices $M_i^{(\lambda)} \in \mathbb{R}^{n \times n}$ are defined recursively for $i = 3, 4, \dots$ by

$$M_{i+2}^{(\lambda)} = \frac{2(i+\lambda)}{i+1} N^{(\lambda)} M_{i+1}^{(\lambda)} - \frac{i+2\lambda-1}{i+1} M_i^{(\lambda)},$$

with $M_1^{(\lambda)} = I$, $M_2^{(\lambda)} = 2\lambda N^{(\lambda)}$ and

$$N^{(\lambda)} = \begin{pmatrix} 0 & \frac{2\lambda}{2(\lambda+1)} & & & \\ \frac{1}{2\lambda} & 0 & \frac{2\lambda+1}{2(\lambda+2)} & & \\ 0 & \frac{2}{2(\lambda+1)} & 0 & \frac{2\lambda+2}{2(\lambda+3)} & \\ & & \frac{2}{2(\lambda+2)} & 0 & \ddots \\ & & & \ddots & \ddots \end{pmatrix}.$$

We now incorporate the non-constant coefficients $\alpha_a(x)$ in the coefficient mapping. Let $\mathbf{a}_a \in \mathbb{R}^n$ denote coefficients of polynomial approximations of $\alpha_a(x)$ in Chebyshev basis for $a = 0$ and in $C^{(a)}$ ultraspherical basis for $a = 1, 2, \dots$. Analogous to Equation (6), we approximate $\mathcal{L}u \approx \sum_{k=1}^n w_k T_k(x)$ by computing the coefficients $\mathbf{w} = (w_1, \dots, w_n)$ defined as

$$\mathbf{w} = \underbrace{(M^{(N)}[\mathbf{a}_N]D_N + S_{N-1}M^{(N-1)}[\mathbf{a}_{N-1}]D_N \cdots + S_{N-1} \cdots S_1 M^{(1)}[\mathbf{a}_1]D_1 + S_{N-1} \cdots S_0 M[\mathbf{a}_0])}_{=L} \mathbf{u}.$$

3.3.2 Three-dimensional differential operators

We now consider the three-dimensional differential operator \mathcal{L} as defined in Equation (2) with non-constant coefficients. We proceed by splitting this operator into one-dimensional operators with non-constant coefficients.

Let the polynomial degree (n_1, n_2, n_3) be chosen sufficiently large to accurately approximate the coefficient functions $\alpha_{abc}(x, y, z)$ using tensorised Chebyshev interpolation in the form of Equation (4). Let $\mathcal{B}^{(abc)} \in \mathbb{R}^{n_1 \times n_2 \times n_3}$ denote the coefficient tensors corresponding to $\alpha_{abc}(x, y, z)$ for each multi-index abc . We define the tensor $\mathcal{A} \in \mathbb{R}^{(N_x+1) \times n_1 \times (N_y+1) \times n_2 \times (N_z+1) \times n_3}$ with entries

$$\mathcal{A}_{(a+1),i,(b+1),j,(c+1),k} = \mathcal{B}_{ijk}^{(abc)}$$

for $0 \leq a \leq N_x$, $0 \leq b \leq N_y$, $0 \leq c \leq N_z$, $1 \leq i \leq n_1$, $1 \leq j \leq n_2$, $1 \leq k \leq n_3$. This approximates the differential operator in the sense that

$$\mathcal{L}u(x, y, z) \approx \tilde{\mathcal{L}}u(x, y, z) = \sum_{a=0}^{N_x} \sum_{i=1}^{n_1} \sum_{b=0}^{N_y} \sum_{j=1}^{n_2} \sum_{c=0}^{N_z} \sum_{k=1}^{n_3} \mathcal{A}_{(a+1),i,(b+1),j,(c+1),k} T_i(x) T_j(y) T_k(z) \frac{\partial^{a+b+c}}{\partial x^a \partial y^b \partial z^c} u(x, y, z).$$

We now reshape \mathcal{A} into a tensor of order 3 in $\mathbb{R}^{(N_x+1)n_1 \times (N_y+1)n_2 \times (N_z+1)n_3}$ and compute a CP decomposition of the form

$$\mathcal{A} = \sum_{r=1}^R \mathbf{a}^{(r)} \circ \mathbf{b}^{(r)} \circ \mathbf{c}^{(r)},$$

where $\mathbf{a}^{(r)} \in \mathbb{R}^{(N_x+1)n_1}$, $\mathbf{b}^{(r)} \in \mathbb{R}^{(N_y+1)n_2}$, $\mathbf{c}^{(r)} \in \mathbb{R}^{(N_z+1)n_3}$. We reshape the vectors $\mathbf{a}_r, \mathbf{b}_r, \mathbf{c}_r$ back into matrices in $\mathbf{A}^{(r)} \in \mathbb{R}^{(N_x+1) \times n_1}$, $\mathbf{B}^{(r)} \in \mathbb{R}^{(N_y+1) \times n_2}$ and $\mathbf{C}^{(r)} \in \mathbb{R}^{(N_z+1) \times n_3}$ respectively. Analogously to Equation (7), we now define one-dimensional differential operators

$$\begin{aligned} \mathcal{L}_r^{(x)} u(x) &= \sum_{a=0}^{N_x} \left(\sum_{i=1}^{n_1} \mathbf{A}_{a+1,i}^{(r)} T_i(x) \right) \frac{\partial^a}{\partial x^a} u(x), \\ \mathcal{L}_r^{(y)} u(y) &= \sum_{b=0}^{N_y} \left(\sum_{j=1}^{n_2} \mathbf{B}_{b+1,j}^{(r)} T_j(y) \right) \frac{\partial^b}{\partial y^b} u(y), \\ \mathcal{L}_r^{(z)} u(z) &= \sum_{c=0}^{N_z} \left(\sum_{k=1}^{n_3} \mathbf{C}_{c+1,k}^{(r)} T_k(z) \right) \frac{\partial^c}{\partial z^c} u(z), \end{aligned}$$

which satisfy by construction

$$\tilde{\mathcal{L}}u(x, y, z) = \sum_{r=1}^R \mathcal{L}_r^{(x)} \mathcal{L}_r^{(y)} \mathcal{L}_r^{(z)} u(x, y, z).$$

Note that the terms of the form $\sum_{i=1}^{n_1} \mathbf{A}_{a+1,i}^{(r)} T_i(x)$ are univariate functions. So, each of the one-dimensional differential operators fits into the setting of Section 3.3.1 and we can obtain matrices $L_r^{(x)}, L_r^{(y)}, L_r^{(z)}$ as in Equation (8).

4 A spectral method for three-dimensional linear PDEs

In this section, we present how to compute approximate solutions for PDEs of the form (3). We again discretize the differential operator \mathcal{L} as in Section 3. Additionally, we discretize the right hand side f using a truncated expansion with ultraspherical basis functions of the form

$$f(x, y, z) \approx \sum_{i=1}^{n_1} \sum_{j=1}^{n_2} \sum_{k=1}^{n_3} \mathcal{F}_{ijk} C_i^{(N_x)}(x) C_j^{(N_y)}(y) C_k^{(N_z)}(z),$$

with coefficient tensor \mathcal{F} . The discretized PDE reads as tensor-valued linear system of the form

$$\sum_{r=1}^R \mathcal{U} \times_1 L_r^{(x)} \times_2 L_r^{(y)} \times_3 L_r^{(z)} = \mathcal{F}. \quad (9)$$

It remains to incorporate the boundary conditions.

4.1 Boundary condition discretization

Following the ideas of [57], we can discretize commonly used boundary conditions for three-dimensional PDEs on cubes as constraints of the form

$$\mathcal{U} \times_1 B_1 = \mathcal{G}_1, \quad \mathcal{U} \times_2 B_2 = \mathcal{G}_2, \quad \mathcal{U} \times_3 B_3 = \mathcal{G}_3, \quad (10)$$

where the matrices $B_1 \in \mathbb{R}^{N_x \times n_1}$, $B_2 \in \mathbb{R}^{N_y \times n_2}$, $B_3 \in \mathbb{R}^{N_z \times n_3}$ have linearly independent rows and $G_1 \in \mathbb{R}^{N_x \times n_2 \times n_3}$, $G_2 \in \mathbb{R}^{n_1 \times N_y \times n_3}$, $G_3 \in \mathbb{R}^{n_1 \times n_2 \times N_z}$. We present two examples how constraints of the form (10) can be derived.

4.1.1 Dirichlet conditions

We consider the Dirichlet boundary condition $u(1, y, z) = h(y, z)$ for a given function $h : [-1, 1] \rightarrow \mathbb{R}$. We approximate the function h using bivariate Chebyshev interpolation in $n_2 \times n_3$ points. Let $H \in \mathbb{R}^{n_2 \times n_3}$ denote the corresponding coefficient tensor. We can enforce that the solution u given in Chebyshev basis (4) coincides with the interpolant of h by demanding that

$$u(1, y, z) = \sum_{i=1}^{n_1} \sum_{j=1}^{n_2} \sum_{k=1}^{n_3} \mathcal{U}_{ijk} T_i(1) T_j(y) T_k(z) = \sum_{j=1}^{n_2} \sum_{k=1}^{n_3} H_{jk} T_j(y) T_k(z). \quad (11)$$

This can be equivalently written as $\mathcal{U} \times_1 B_1 = G_1$ with $B = (T_1(1), \dots, T_{n_1}(1))$ and $\mathcal{G}_1(1, :, :) = H$.

We now consider an additional Dirichlet boundary condition $u(-1, y, z) = \tilde{h}$. Again, we compute the coefficient tensor \tilde{H} corresponding to \tilde{h} . Analogously to Equation (11), we enforce that $u(-1, y, z)$ coincides with the interpolant of \tilde{h} . We can express both conditions simultaneously in the form of (10) by defining

$$B_1 = \begin{pmatrix} T_1(-1) & T_2(-1) & \dots & T_n(-1) \\ T_1(1) & T_2(1) & \dots & T_n(1) \end{pmatrix},$$

and $\mathcal{G}_1(1, :, :) = \tilde{H}$, $\mathcal{G}_2(2, :, :) = H$.

4.1.2 Neumann conditions

We consider the Neumann boundary condition $\frac{\partial}{\partial x} u(1, y, z) = h(y, z)$ for a given function h and $u \in \mathbb{P}_{n_1 n_2 n_3}$ represented in Chebyshev basis (4). As in the Dirichlet case, we use bivariate Chebyshev interpolation h to obtain the coefficient tensor $H \in \mathbb{R}^{n_2 \times n_3}$. We now demand that

$$\frac{\partial}{\partial x} u(1, y, z) = \sum_{i=1}^{n_1} \sum_{j=1}^{n_2} \sum_{k=1}^{n_3} (\mathcal{U} \times_1 (S_0^{-1} D_1))_{ijk} T_i(1) T_j(y) T_k(z) = \sum_{j=1}^{n_2} \sum_{k=1}^{n_3} H_{jk} T_j(y) T_k(z), \quad (12)$$

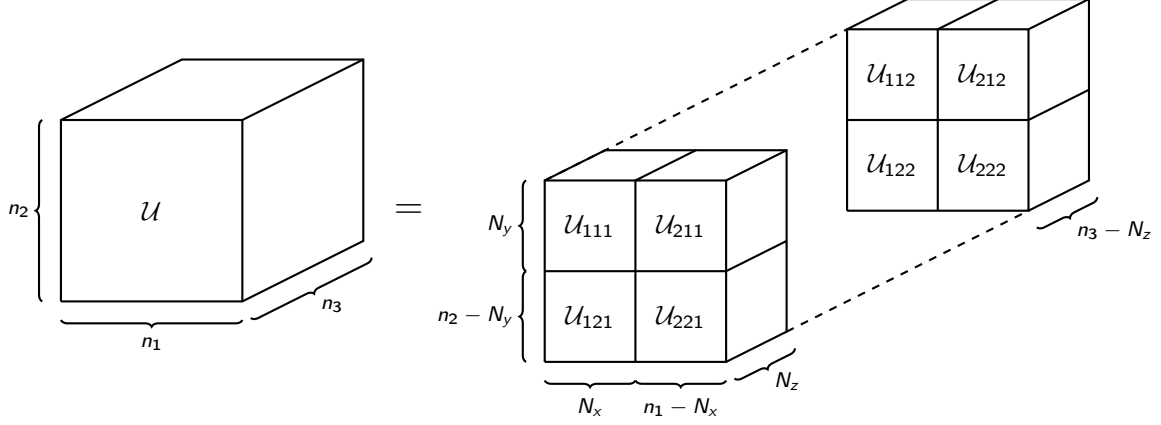


Figure 1: Visualization of the block decomposition of $\mathcal{U} \in \mathbb{R}^{n_1 \times n_2 \times n_3}$ with block $\mathcal{U}_{111} \in \mathbb{R}^{N_x \times N_y \times N_z}$.

where S_0, D_1 are the transformation matrices defined in Section 3.3.1 such that $\mathcal{U} \times_1 (S_0^{-1} D_1)$ contains the Chebyshev coefficients of $\frac{\partial}{\partial x} u$. Equation (12) can be expressed in the form of (10) with $B_1 = (T_1(1), \dots, T_{n_1}(1)) S_0^{-1} D_1$ and $\mathcal{G}_1(1, :, :) = H$.

4.2 Incorporating the boundary conditions

We need to incorporate the discretized boundary conditions (10) into the discretized PDE (9) to obtain the unique solution \mathcal{U} . Following the ideas of [57, Section 6], we compute \mathcal{U} by substituting (10) into (9).

Since B_1, B_2, B_3 have linearly independent rows, we can assume without loss of generality that

$$B_1(1: N_x, 1: N_x) = I, \quad B_2(1: N_y, 1: N_y) = I, \quad B_3(1: N_z, 1: N_z) = 1. \quad (13)$$

Substituting these boundary conditions leads to

$$\begin{aligned} & \sum_{r=1}^R \mathcal{U} \times_1 \underbrace{(L_r^{(x)} - L_r^{(x)}(:, 1: N_x) B_1)}_{=\tilde{L}_r^{(x)}} \times_2 \underbrace{(L_r^{(y)} - L_r^{(y)}(:, 1: N_y) B_2)}_{=\tilde{L}_r^{(y)}} \times_3 \underbrace{(L_r^{(z)} - L_r^{(z)}(:, 1: N_z) B_3)}_{=\tilde{L}_r^{(z)}} = \\ & \mathcal{F} - \sum_{r=1}^R G_1 \times_1 L_r^{(x)}(:, 1: N_x) \times_2 L_r^{(y)} \times_3 L_r^{(z)} \\ & - \sum_{r=1}^R G_2 \times_1 (L_r^{(x)} - L_r^{(x)}(:, 1: N_x) B_1) \times_2 L_r^{(y)}(:, 1: N_y) \times_3 L_r^{(z)} \\ & - \sum_{r=1}^R G_3 \times_1 (L_r^{(x)} - L_r^{(x)}(:, 1: N_x) B_1) \times_2 (L_r^{(y)} - L_r^{(y)}(:, 1: N_y) B_2) \times_3 L_r^{(z)}(:, 1: N_z), \end{aligned}$$

where we denote the right hand side by $\tilde{\mathcal{F}}$. Observe that the first N_x, N_y, N_z columns of $\tilde{L}_r^{(x)}, \tilde{L}_r^{(y)}, \tilde{L}_r^{(z)}$ are zero due assumption (13). Let \mathcal{U} be decomposed into tensor blocks as described in Figure 1. The system after substitution uniquely determines the block $\mathcal{U}_{222} = \mathcal{U}((N_x + 1): n_1, (N_y + 1): n_2, (N_z + 1): n_3)$, which

can be written as

$$\begin{aligned} & \sum_{r=1}^R \mathcal{U}_{222} \times_1 \underbrace{\tilde{L}_r^{(x)}(1: (n_1 - N_x), (N_x + 1): n_1)}_{=\hat{L}_r^{(x)}} \times_2 \underbrace{\tilde{L}_r^{(y)}(1: (n_2 - N_y), (N_y + 1): n_2)}_{=\hat{L}_r^{(y)}} \\ & \times_3 \underbrace{\tilde{L}_r^{(z)}(1: (n_3 - N_z), (N_z + 1): n_3)}_{=\hat{L}_r^{(z)}} = \underbrace{\tilde{\mathcal{F}}(1: (n_1 - N_x), 1: (n_2 - N_y), 1: (n_3 - N_z))}_{=\hat{\mathcal{F}}}. \end{aligned} \quad (14)$$

The remaining blocks can be reconstructed from the discretized boundary conditions (10) as

$$\begin{aligned} \mathcal{U}_{122} &= G_1 - \mathcal{U}_{222} \times_1 B_1, & \mathcal{U}_{212} &= G_2 - \mathcal{U}_{222} \times_2 B_2, \\ \mathcal{U}_{221} &= G_3 - \mathcal{U}_{222} \times_3 B_3, & \mathcal{U}_{112} &= G_1 - \mathcal{U}_{212} \times_1 B_1, \\ \mathcal{U}_{121} &= G_1 - \mathcal{U}_{221} \times_1 B_1, & \mathcal{U}_{211} &= G_3 - \mathcal{U}_{212} \times_3 B_3, \\ \mathcal{U}_{111} &= G_1 - \mathcal{U}_{211} \times_1 B_1. \end{aligned}$$

4.3 Solving tensor-valued linear systems

The computation of \mathcal{U} requires the solution of the unconstrained tensor-valued linear system (14) of the form

$$\sum_{r=1}^R \mathcal{U}_{222} \times_1 \hat{L}_r^{(x)} \times_2 \hat{L}_r^{(y)} \times_3 \hat{L}_r^{(z)} = \hat{\mathcal{F}}. \quad (15)$$

This system can be solved by reshaping the tensor-valued linear system into a vector-valued linear system of the form

$$\left(\sum_{r=1}^R \hat{L}_r^{(z)} \otimes \hat{L}_r^{(y)} \otimes \hat{L}_r^{(x)} \right) \text{vec}(\mathcal{U}_{222}) = \text{vec}(\hat{\mathcal{F}}), \quad (16)$$

where \otimes denotes the Kronecker product and $\text{vec}(\cdot)$ denotes the vectorization [36].

For certain PDEs we can transform the system (15) into a Laplace-like equation

$$\mathcal{U}_{222} \times_1 U + \mathcal{U}_{222} \times_2 V + \mathcal{U}_{222} \times_3 W = \check{\mathcal{F}}, \quad (17)$$

with matrices $U \in \mathbb{R}^{(n_1 - N_x) \times (n_1 - N_x)}$, $V \in \mathbb{R}^{(n_2 - N_y) \times (n_2 - N_y)}$, $W \in \mathbb{R}^{(n_3 - N_z) \times (n_3 - N_z)}$ and tensor $\check{\mathcal{F}} \in \mathbb{R}^{(n_1 - N_x) \times (n_2 - N_y) \times (n_3 - N_z)}$. For instance, this can be achieved for $N_x = N_y = N_z$, $n_1 = n_2 = n_3$ and $B_1 = B_2 = B_3$, when there exists a CP decomposition of the tensor \mathcal{A} defined in Section 3 with symmetry constraints [8] of the form

$$\mathcal{A} = \mathbf{a} \circ \mathbf{v} \circ \mathbf{w} + \mathbf{u} \circ \mathbf{b} \circ \mathbf{w} + \mathbf{u} \circ \mathbf{v} \circ \mathbf{c}. \quad (18)$$

Then then Equation (15) is equivalent to the Laplace-like equation (17) with

$$\begin{aligned} U &= (\hat{\mathcal{L}}_1^{(y)})^{-1} \hat{\mathcal{L}}_1^{(x)}, & V &= (\hat{\mathcal{L}}_2^{(x)})^{-1} \hat{\mathcal{L}}_2^{(y)}, & W &= (\hat{\mathcal{L}}_3^{(x)})^{-1} \hat{\mathcal{L}}_3^{(z)}, \\ \check{\mathcal{F}} &= \hat{\mathcal{F}} \times_1 (\hat{\mathcal{L}}_1^{(y)})^{-1} \times_2 (\hat{\mathcal{L}}_2^{(x)})^{-1} \times_3 (\hat{\mathcal{L}}_3^{(x)})^{-1}. \end{aligned} \quad (19)$$

To solve Laplace-like equations (17), we apply the recursive blocked algorithm developed in [9]. It transforms the matrices U, V, W into quasi-triangular form by computing Schur decompositions. Block decompositions for the quasi-triangular matrices reveal an equivalent system of Laplace-like equations with smaller matrices. Applying this observation recursively, until we can solve the small Laplace-like equations efficiently by reshaping, yields the blocked recursive algorithm. For $n = n_1 = n_2 = n_3$ this approach has a theoretical runtime of $\mathcal{O}(n^4)$ operations. In Section 5.1, we demonstrate that this recursive blocked algorithm is much faster than directly reshaping the tensor-valued linear system.

5 Numerical results

All numerical experiments in this section were performed in MATLAB R2018b on a Lenovo Thinkpad T480s with Intel Core i7-8650U CPU and 15.4 GiB RAM. The code to reproduce these results is available from <https://github.com/cstroessner/SpectralMethod3D>.

5.1 Runtime comparison

We consider Poisson’s equation $\Delta u = f$ with homogeneous Dirichlet boundary conditions. In Table 1, we compare our global spectral method to the nested alternating direction implicit method (NADIM) proposed in [22, Section 5].

	$n = 10$		$n = 30$		$n = 50$		$n = 150$	
	Time	Error	Time	Error	Time	Error	Time	Error
NADIM	15.2	$1.47 \cdot 10^{-5}$	611	$1.85 \cdot 10^{-8}$	-	-	-	-
reshape	0.010	$1.80 \cdot 10^{-5}$	1.6	$9.44 \cdot 10^{-16}$	69.8	$1.22 \cdot 10^{-15}$	-	-
recursive	0.081	$1.80 \cdot 10^{-5}$	0.076	$2.59 \cdot 10^{-13}$	0.22	$2.21 \cdot 10^{-12}$	9.21	$5.76 \cdot 10^{-11}$

Table 1: Comparison of algorithms to solve Poisson’s equation with known solution $u^*(x, y, z) = \sin(\pi x) \sin(\pi y) \sin(\pi z)$. To compute solutions $u \in \mathbb{P}_{n,n,n}$ with our global spectral method we compare reshaping (14) and solving (16) with backslash in Matlab (reshape) to transforming (14) into a Laplace-like equation (17) and solving with the blocked recursive solver [9] (recursive). Additionally, we compare to NADIM [22]. For various n , we measure the runtime in seconds and we estimate $\|u - u^*\|_\infty$, where $\|\cdot\|_\infty$ denotes the uniform norm, by sampling 1 000 random points.

We observe that even though NADIM has an asymptotic runtime of $\mathcal{O}(n^3(\log(n))^3)$ [22], it is the slowest algorithm in our setting and can not handle $n > 30$ in a reasonable amount of time. The asymptotic runtime of the recursive algorithm is slower with $\mathcal{O}(n^4)$, but in our experiments it is the fastest method and it can handle values of up to $n = 150$ in less than 10 seconds. For $n = 50$ solving the reshaped system (16) with backslash leads to an error of order 10^{-15} , whereas the recursive algorithm only achieves an error of order 10^{-13} . While the recursive algorithm is able to solve much larger systems, it is slightly more sensitive to numerical rounding errors.

5.2 Stationary problems

5.2.1 Helmholtz problems

We consider the Helmholtz equation as in [28, 57], which arises for instance in the context of three-dimensional wave equations in acoustics [63] and seismic-imaging [49]. It is defined as

$$\Delta u(x, y, z) + \kappa^2 u(x, y, z) = f(x, y, z),$$

for suitable Dirichlet boundary conditions on $[-1, 1]^3$ and coefficient $\kappa \in \mathbb{R}$. For this differential operator, we define the tensor \mathcal{A} as in Section 3.2. We observe that a CP decomposition in the form (18) is given by

$$\mathcal{A} = \begin{pmatrix} \kappa^2 \\ 0 \\ 1 \end{pmatrix} \circ \begin{pmatrix} 1 \\ 0 \\ 0 \end{pmatrix} \circ \begin{pmatrix} 1 \\ 0 \\ 0 \end{pmatrix} + \begin{pmatrix} 1 \\ 0 \\ 0 \end{pmatrix} \circ \begin{pmatrix} 0 \\ 0 \\ 1 \end{pmatrix} \circ \begin{pmatrix} 1 \\ 0 \\ 0 \end{pmatrix} + \begin{pmatrix} 1 \\ 0 \\ 0 \end{pmatrix} \circ \begin{pmatrix} 1 \\ 0 \\ 0 \end{pmatrix} \circ \begin{pmatrix} 0 \\ 0 \\ 1 \end{pmatrix}. \quad (20)$$

Hence, we can derive a Laplace-like structure (17) for Equation (14) and employ the recursive solver.

In the following, we employ the global spectral method for the Helmholtz equation in [7, Section 5.3] given by

$$\Delta u(x, y, z) + \kappa(x)^2 u(x, y, z) = f(x, y, z), \quad (21)$$

with function $\kappa(x) = a - b \cos(\pi cx/2)$ and coefficients $a, b, c \in \mathbb{R}$. The right hand side f and the Dirichlet boundary conditions are chosen to correspond to the solution

$$u^*(x, y, z) = \exp(-\kappa(x)/c) \cos(\pi ay/2) \cos(\pi bz/2). \quad (22)$$

In order to incorporate the coefficient function $\kappa(x)$, we compute one-dimensional differential operators as in Equation (7) from the CP-decomposition (20). We then set $\mathcal{L}_1^{(x)}u(x) = \kappa(x)^2u(x) + \frac{\partial^2}{\partial x^2}u(x)$ and discretize this operator as described in Section 3.3.1. The resulting equation (14) can still be transformed into a Laplace-like equation (17) by setting $U, V, W, \tilde{\mathcal{F}}$ as defined in (19).

In Figure 2, we depict how well the solution $u \in \mathbb{P}_{n,n,n}$ of our global spectral method approximates u^* . We compare to the trivariate Chebyshev interpolant \tilde{u} of u^* , which is close to the best approximation of u in $\mathbb{P}_{n,n,n}$ and converges quickly [15, 60]. For $n < 80$ the solution u and the interpolant \tilde{u} almost coincide. But for $n > 80$ the error $\|u - u^*\|_\infty$ stagnates, whilst the interpolation error $\|\tilde{u} - u^*\|_\infty$ continues to decrease further before reaching a plateau close to machine precision. This discrepancy is caused by the higher sensitivity of the recursive blocked solver to numerical rounding errors, which we already observed in Table (1).

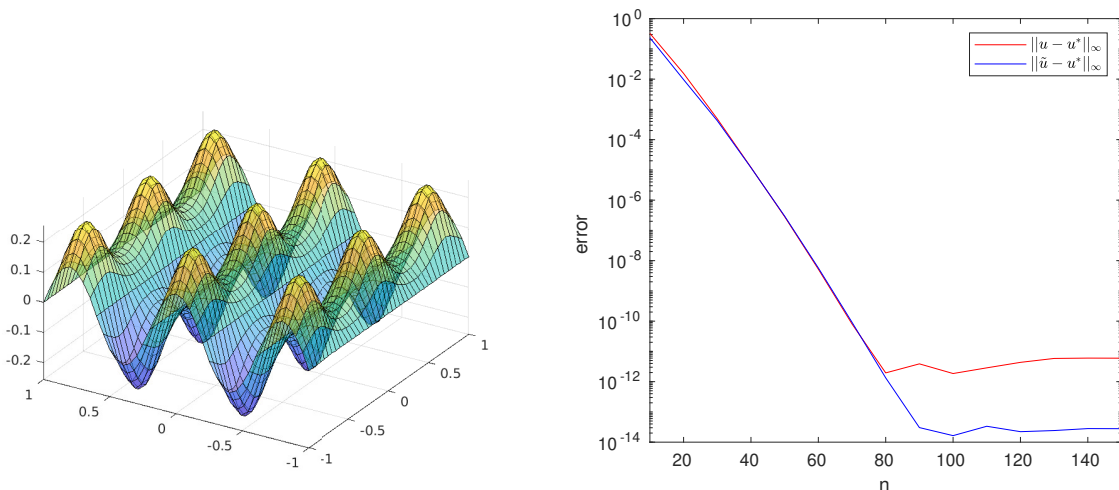


Figure 2: Left: We plot $u^*(x, y, z)$ as defined in (22) for $(a, b, c) = (5, 3, 5)$ and fixed $z = 1/4$. Right: We solve the Helmholtz equation (21) for $(a, b, c) = (5, 3, 5)$ with known solution u^* (22) via our global spectral method to obtain the solution $u \in \mathbb{P}_{n,n,n}$ for various n . Further, we compute the trivariate Chebyshev interpolant $\tilde{u} \in \mathbb{P}_{n,n,n}$ of u^* . For each n , we estimate $\|u - u^*\|_\infty$ and $\|\tilde{u} - u^*\|_\infty$ using 1000 sample points (evaluation error).

Remark. The derivation of the Laplace-like system from the CP decomposition can be extended from the Helmholtz equation to convection diffusion problems of the form

$$-\nu \Delta u + \mathbf{c}^T \nabla u = f,$$

with $\nu \in \mathbb{R}$ and $\mathbf{c} \in \mathbb{R}^3$ as studied in [4, 10, 65]. For these problems we define the CP-decomposition

$$\mathcal{A} = \begin{pmatrix} 0 \\ \mathbf{c}_1 \\ -\nu \end{pmatrix} \circ \begin{pmatrix} 1 \\ 0 \\ 0 \end{pmatrix} \circ \begin{pmatrix} 1 \\ 0 \\ 0 \end{pmatrix} + \begin{pmatrix} 1 \\ 0 \\ 0 \end{pmatrix} \circ \begin{pmatrix} 0 \\ \mathbf{c}_2 \\ -\nu \end{pmatrix} \circ \begin{pmatrix} 1 \\ 0 \\ 0 \end{pmatrix} + \begin{pmatrix} 1 \\ 0 \\ 0 \end{pmatrix} \circ \begin{pmatrix} 1 \\ 0 \\ 0 \end{pmatrix} \circ \begin{pmatrix} 0 \\ \mathbf{c}_3 \\ -\nu \end{pmatrix}.$$

5.2.2 Diffusion problems with separable coefficient

Diffusion problems of the form

$$-\nabla \cdot (a(x, y, z) \nabla u(x, y, z)) = f(x, y, z), \quad (23)$$

with a separable coefficient $a(x, y, z) = a_1(x)a_2(y)a_3(z)$ defined by univariate functions $a_1, a_2, a_3 : [-1, 1] \rightarrow \mathbb{R}$, are not directly given as linear partial differential operator of the form (2). We can, however, decompose the three-dimensional differential operator into a sum of three differential operators similar to (7) as

$$\nabla \cdot (a(x, y, z) \nabla u(x, y, z)) = \underbrace{\left(\frac{\partial}{\partial x} (a(x, y, z) \frac{\partial}{\partial x}) \right)}_{=\tilde{\mathcal{L}}_1^{(x)}} + \underbrace{\left(\frac{\partial}{\partial y} (a(x, y, z) \frac{\partial}{\partial y}) \right)}_{=\tilde{\mathcal{L}}_2^{(y)}} + \underbrace{\left(\frac{\partial}{\partial z} (a(x, y, z) \frac{\partial}{\partial z}) \right)}_{=\tilde{\mathcal{L}}_3^{(z)}} u(x, y, z).$$

Applying the differential operator $\tilde{\mathcal{L}}_1^{(x)}$ to a polynomial $u \in \mathbb{P}_{n,n,n}$ can be written analogously to (8) as

$$\mathcal{V} = \mathcal{U} \times_1 \underbrace{S_1 D_1 S_1^{-1} M^{(1)}[\mathbf{a}_1] D_1}_{=L_1^{(x)}} \times_2 \underbrace{M^{(2)}[\mathbf{a}_2] S_1 S_0}_{=L_1^{(y)}} \times_3 \underbrace{M^{(2)}[\mathbf{a}_3] S_1 S_0}_{=L_1^{(z)}}$$

where $\mathbf{a}_1 \in \mathbb{R}^{n_1}$, $\mathbf{a}_2 \in \mathbb{R}^{n_2}$, $\mathbf{a}_3 \in \mathbb{R}^{n_3}$ denote the coefficients for univariate Chebyshev interpolation of a_1, a_2, a_3 as in Section 3.3.1. The multiplication matrices $M[\mathbf{a}]$, differentiation matrices D_1 and transformation matrices S_0, S_1 are defined as in Section 3. We obtain analogous discretizations for $\tilde{\mathcal{L}}_2^{(y)}$ and $\tilde{\mathcal{L}}_3^{(z)}$. Observe that the discretization has the same symmetric structure as the CP decomposition (18). Thus, we can transform (14) to a Laplace-like equation (17) by defining $U, V, W, \check{\mathcal{F}}$ as in (19) and use the recursive solver.

5.2.3 Diffusion problems with higher rank coefficient

Most diffusion problems (23) arising in the study of groundwater flow and uncertainty quantification [12, 23, 40, 51, 55, 61] do not have a rank-1 coefficients $a(x, y, z)$. The coefficient is often given by a truncated expansion as sum of separable functions of the form

$$a(x, y, z) = \sum_{r=1}^{R_a} a_1^{(r)}(x) a_2^{(r)}(y) a_3^{(r)}(z),$$

with $R_a > 1$ and univariate functions $a_1^{(r)}, a_2^{(r)}, a_3^{(r)} : [-1, 1] \rightarrow \mathbb{R}$. The PDE (23) can now be written as

$$-\sum_{r=1}^{R_a} \nabla \cdot (a_1^{(r)}(x) a_2^{(r)}(y) a_3^{(r)}(z) \nabla u(x, y, z)) = f(x, y, z). \quad (24)$$

Following the ideas in Section 5.2.2, we can discretize (23) for each separable function $a_1^{(r)}(x) a_2^{(r)}(y) a_3^{(r)}(z)$. Adding these discretizations yields a discretization of the form (9) with $R = 3R_a$. Since $R > 3$, we can not find a Laplace-like formulation of (14) and we can not use the recursive solver.

We can, however, use preconditioned GMRES [24] to compute solutions of (14) seen as linear system. Through out this work we restart GMRES every 15 iterations. As preconditioner we employ the recursive solver to solve Equation (14) for a discretization of the same diffusion problem (24) with with the coefficient $a(x, y, z)$ replaced by a separable coefficient $b(x, y, z)$.

From now on, we consider the rank-2 coefficient $a(x, y, z) = (1 + x^2)(1 + y^2)(1 + z^2) + \exp(x + y + z)$. We use our global spectral method with $n = n_1 = n_2 = n_3 = 30$ to solve the Diffusion problem (24) with known solution $u^*(x, y, z) = \sin(\pi x) \sin(\pi y) \sin(\pi z)$ and Dirichlet boundary conditions. In Figure 3, we display the convergence rates for GMRES with preconditioners based on the constant coefficient $b_1(x, y, z) = \|a(x, y, z)\|_{\mathcal{L}^2}$ and the separable coefficient $b_2(x, y, z) = (1 + x^2)(1 + y^2)(1 + z^2)$. Both preconditioners yield solutions u , for which the error $\|u - u^*\|_{\infty}$ is close to machine precision. Solving with b_1 takes 4.54 seconds. For separable coefficient b_2 fewer iterations are necessary and the computation only takes 2.04 seconds. For comparison, reshaping as in Section 5.1 would take 77.0 seconds.

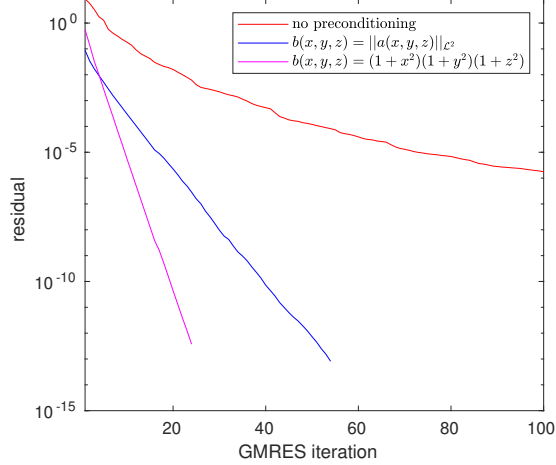


Figure 3: Convergence rate of preconditioned GMRES for solving Equation (14) for the Diffusion problem (24) with coefficient $a(x, y, z) = (1+x^2)(1+y^2)(1+z^2) + \exp(x+y+z)$. We compare no preconditioning and preconditioning with a separable coefficient $b(x, y, z)$ as described in Section 5.2.3.

5.2.4 Helmholtz equation with non-constant coefficients

As final stationary problem, we study a variable coefficient Helmholtz equation as in [57, Example 2]. We consider the PDE

$$\Delta u(x, y, z) + \kappa(x, y, z)u(x, y, z) = f(x, y, z),$$

with function $\kappa(x, y, z) = \cos(x+y+z)$. For $n = n_1 = n_2 = n_3 = 30$, we compute a discretization (9) by computing a CP decomposition of \mathcal{A} as defined as in Section 3.3.2 using the Levenberg-Marquardt method [41, Algorithm 3.16] with $R = 6$. This leads to a discretized PDE, for which we solve Equation (14) with preconditioned GMRES with restarting as in Section (5.2.3). In the preconditioner we solve Equation (14) for the Helmholtz equation (21) with constant coefficient $\kappa = \|\kappa(x, y, z)\|_{\mathcal{L}^2}$.

When the right hand side and Dirichlet boundary conditions are chosen to match the known solution $u^*(x, y, z) = \sin(\pi x) \sin(\pi y) \sin(\pi z)$, solving with preconditioned GMRES takes 0.44 seconds. The computed solution u satisfies $\|u - u^*\|_{\infty} \approx 3.3 \cdot 10^{-14}$, where we estimate the uniform norm using 1 000 sample points.

Remark. Here, the main computational bottleneck is computing the CP decomposition of $\mathcal{A} \in \mathbb{R}^{90 \times 90 \times 90}$, which takes 61 minutes. For the Helmholtz equation a similar splitting of the PDE in the form of (7) can be constructed from a CP decomposition of the coefficient tensor in $\mathbb{R}^{30 \times 30 \times 30}$ obtained from Chebyshev interpolation of $\kappa(x, y, z)$. This CP decomposition leads to a discretization of the operator $\kappa(x, y, z)\mathcal{I}$, which can be added to a discretization of the Laplacian. The rank-3 CP decomposition of this smaller tensor only takes 15.5 seconds. In Section 5.4, we use this approach of adding discretizations.

5.3 Time-dependent problems

In this section, we introduce an implicit Euler scheme to solve parabolic PDEs of the form

$$\frac{\partial}{\partial t} u(x, y, z, t) + \mathcal{L}u(x, y, z, t) = 0,$$

where \mathcal{L} is a linear partial differential operator acting only on the spatial variables x, y, z . The system is complemented with boundary conditions. We are interested in the time evolution starting from a given initial function $u(x, y, z, 0) = u_0(x, y, z)$. We discretize the equation in time using the uniform step length h . For each $\tau = 1, 2, \dots$, we compute $u_{\tau}(x, y, z) \approx u(x, y, z, \tau h)$ as solution of the stationary linear PDE

$$(\mathcal{I} - h\mathcal{L})u_{\tau+1} = u_{\tau}. \quad (25)$$

We approximate each function u_τ by a polynomial of the form 4 represented by the coefficient tensor \mathcal{U}_τ . The initial \mathcal{U}_0 is computed via tensorised Chebyshev interpolation. For $\tau = 1, 2, \dots$, we obtain \mathcal{U}_τ by applying our spectral method to solve Equation (25). We discretize the operator $(\mathcal{I} - h\mathcal{L})$ directly like the Helmholtz equation in Section 5.2.1. This allows us to employ the recursive solver. Note that the right hand side is represented in terms of an ultraspherical basis. Hence, the computation of \mathcal{U}_τ requires multiplying $\mathcal{U}_{\tau-1}$ with appropriate basis transformation matrices.

We demonstrate this implicit Euler scheme for the parabolic PDE studied in [62, Section 6.1]. The function $u^*(x, y, z, t) = \exp(-3\pi^2 t) \sin(\pi x) \sin(\pi y) \sin(\pi z)$ satisfies the parabolic PDE

$$\frac{\partial}{\partial t} u + \Delta u = 0,$$

on the domain $[-1, 1]^3$ with homogeneous Dirichlet boundary conditions. We use an implicit Euler scheme for $u_0(x, y, z) = \sin(\pi x) \sin(\pi y) \sin(\pi z)$ and compare our global spectral method to a finite difference method. In each timestep of the finite difference method, we solve a linear system with a sparse Kronecker-structured finite difference matrix using the backslash operator in MATLAB.

The time evolution of the errors is displayed in Figure 4. We observe that for $n = 20$ and $h = 10^{-2}$ both approximations lead to very similar errors, but the computation time for 50 implicit Euler steps decreases from 5.32 seconds for the finite difference method to 0.82 seconds for our global spectral method. In this case the error is dominated by the implicit Euler scheme for both methods. In contrast, for $n = 30$ and $h = 10^{-4}$, the errors for the spectral method are smaller. For large τ the error of both approaches is dominated by the time discretization via the implicit Euler scheme. However, in the initial 750 time steps the error of the spatial discretization dominates for the finite difference scheme, whereas the global spectral method is able to represent u_τ accurately.

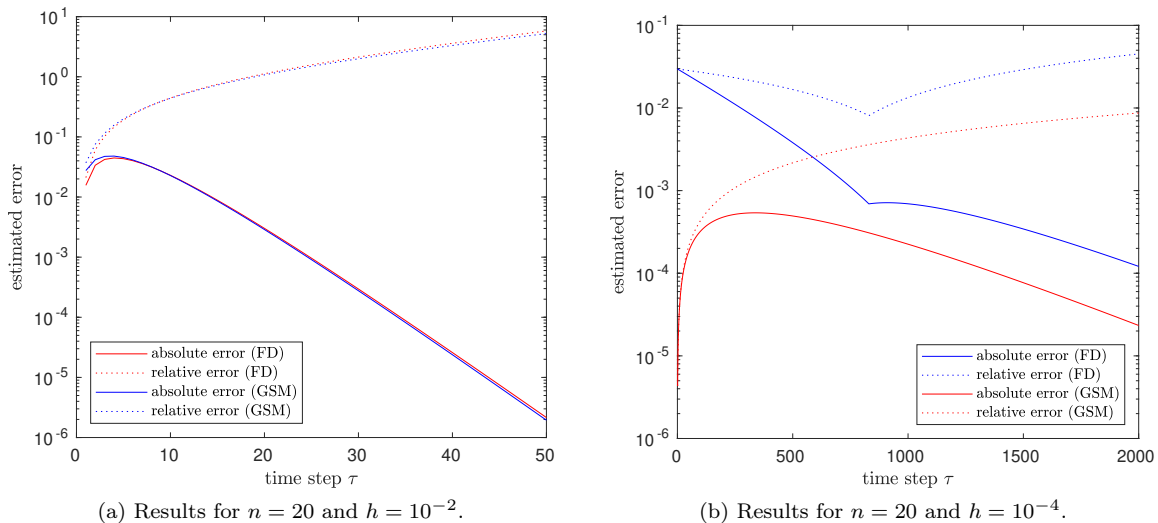


Figure 4: Error plots for the parabolic PDE example in Section 5.3. We apply an implicit Euler scheme to compute approximations $u_\tau(x, y, z) \approx u(x, y, z, \tau h)$ and compare the solutions for the global spectral method (GSM) with solutions in $\mathbb{P}_{n,n,n}$ and a finite difference discretization (FD) on a regular $n \times n \times n$ grid. The absolute error $\|u^*(x, y, z, \tau h) - u_\tau(x, y, z)\|_\infty$ is estimated in each timestep from evaluations at 100 sample points. The relative error is computed from the estimation of the absolute error.

Remark. The methods presented in this work can also be used to solve two-dimensional parabolic PDEs on rectangles by treating the time as third space variable in the discretization of the operator. We refer to [57] for more details on this approach.

5.4 Eigenvalue problems

The methods presented in this work can be extended to solve PDE eigenvalue problems, in which we search eigenvalues λ and eigenfunctions u satisfying the equation $\mathcal{L}u = \lambda u$ complemented with homogeneous Dirichlet boundary conditions. We are particularly interested in finding the eigenvalue with minimal absolute value. For this purpose we employ the inverse iteration algorithm [24]. Starting from an initial function u_0 we iteratively compute an approximation of the eigenfunction. For $t = 1, 2, \dots$, we compute u_t as solution of the PDE

$$\mathcal{L}u_t = \frac{u_{t-1}}{\|u_{t-1}\|_{\mathcal{L}^2}}. \quad (26)$$

We approximate the eigenvalue using the Rayleigh quotient $\frac{1}{\lambda} \approx \frac{\langle u_{t-1}, u_t \rangle}{\langle u_{t-1}, u_{t-1} \rangle}$, where $\langle \cdot, \cdot \rangle$ denotes the standard \mathcal{L}^2 scalar product. We again proceed by discretizing the differential operator and the function u to solve Equation (26) using the spectral method introduced in Section 4.

Let the functions $u, v \in \mathbb{P}_{n_1, n_2, n_3}$ be given in the form of (4). We evaluate the norm as $\|u\|_{\mathcal{L}^2} = \langle u, u \rangle$ and the scalar product $\langle u, v \rangle$ by interpolating the function uv using tensorised Chebyshev polynomial basis functions as in [15, 42]. In a second step, we integrate the approximation of uv using the exact values for the integrals of the basis functions [60, Theorem 19.2].

We test our method for the elliptic PDE eigenvalue problem

$$-\Delta u(x, y, z) + v(x, y, z)u(x, y, z) = \lambda u(x, y, z), \quad (27)$$

with potential $v(x, y, z) = \sin(\pi/2(x + 1))\sin(\pi/2(y + 1))\sin(\pi/2(z + 1))$ as in [38, 27]. Due to the potential $v(x, y, z)$ the inverse iteration steps (26) are Helmholtz equations (21) with non-constant, separable coefficients. We discretize these by adding a discretization with $R = 1$ of $v(x, y, z)\mathcal{I}$ to a discretization of the Laplacian. The resulting discretized PDE (9) has $R = 4$ and we apply preconditioned GMRES with restarting using a Helmholtz equation with constant coefficient $\|v(x, y, z)\|_{\mathcal{L}^2}$ to compute solutions as in Section 5.2.4. We compare our global spectral method to a finite difference scheme on a regular grid for solving (26). In Figure 5 we observe that the eigenvalues computed as Rayleigh coefficients converge at a much faster rate for the global spectral method compared to the finite difference approach. Already for $n = 20$ the global spectral method reaches an error close to machine precision.

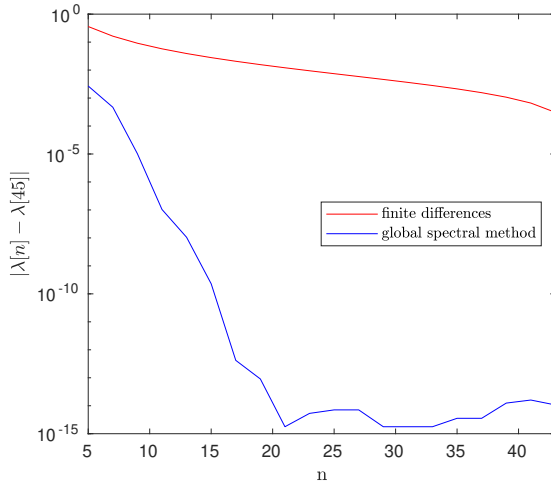


Figure 5: Eigenvalue convergence rate for the PDE eigenvalue problem (27) computed as Rayleigh coefficients from u_{50} in the inverse iteration method, where the solutions u_t are computed via the global spectral method with $u_t \in \mathbb{P}_{n,n,n}$ and a finite difference method on a regular $n \times n \times n$ grid. We denote the eigenvalue obtained for n by $\lambda[n]$. For both algorithms we plot $|\lambda[n] - \lambda[45]|$ since the exact λ is not known.

Remark. We would like to point out that our approach can be used to compute a basis for the (continuous) Krylov subspace, which is used in the Arnoldi method [1, 24] and in the Least-squares spectral method in [29].

6 Conclusions

In this work, we derive a global spectral method for solving three-dimensional linear PDEs on cubes with very high accuracy. We demonstrate that the Laplace-like equations arising for certain PDEs can be solved efficiently with the blocked recursive solver [9]. Our numerical experiments show that applying this solver directly or as preconditioner vastly outperforms all existing methods. The versatility of our method is presented by the extension to eigenvalue and time-dependent problems.

Future work. The computational complexity of our global spectral method is heavily influenced by the storage needed to store the full coefficient tensors \mathcal{U} and \mathcal{F} for representing the solution and right-hand side, respectively. For certain problems these tensors admit good low-rank approximations. Applying such approximations leads to so called functional low-rank approximations [6, 15, 25, 30, 53], which have the potential to drastically reduce the storage complexity. Exploiting this potential requires determining suitable approximation formats and using a specialized solver for the chosen formats. For instance, in [52] it is shown that under certain conditions the solution of Laplace-like equations (17) can be represented in tensor train or Tucker format when the right hand side is given in the same format. The functional tensor train format [6, 11, 25, 53], could potentially be used to extend the global spectral method to higher dimensional, linear PDEs on hypercubes. The computational complexity of time-dependent problems could be reduced using rank-adaptive, dynamical low-rank approximations [3, 13, 14, 35].

References

- [1] W. E. ARNOLDI, *The principle of minimized iteration in the solution of the matrix eigenvalue problem*, Quart. Appl. Math., 9 (1951), pp. 17–29.
- [2] I. BABUŠKA AND M. SURI, *The p - and h - p versions of the finite element method, an overview*, Comput. Methods Appl. Mech. Engrg., 80 (1990), pp. 5–26. Spectral and high order methods for partial differential equations (Como, 1989).
- [3] M. BACHMAYR, H. EISENMANN, E. KIERI, AND A. USCHMAJEV, *Existence of dynamical low-rank approximations to parabolic problems*, Math. Comp., 90 (2021), pp. 1799–1830.
- [4] J. BALLANI AND L. GRASEDYCK, *A projection method to solve linear systems in tensor format*, Numer. Linear Algebra Appl., 20 (2013), pp. 27–43.
- [5] Y. BAZILEVS, M.-C. HSU, J. KIENDL, R. WÜCHNER, AND K.-U. BLETZINGER, *3D simulation of wind turbine rotors at full scale. Part II: Fluid–structure interaction modeling with composite blades*, Int. J. Numer. Meth. Fluids, 65 (2010), pp. 236–253.
- [6] D. BIGONI, A. P. ENGSIG-KARUP, AND Y. M. MARZOUK, *Spectral tensor-train decomposition*, SIAM J. Sci. Comput., 38 (2016), pp. A2405–A2439.
- [7] L. F. CANINO, J. J. OTTUSCH, M. A. STALZER, J. L. VISHER, AND S. M. WANDZURA, *Numerical solution of the Helmholtz equation in 2D and 3D using a high-order Nyström discretization*, J. Comput. Phys., 146 (1998), pp. 627–663.
- [8] J. D. CARROLL, S. PRUZANSKY, AND J. B. KRUSKAL, *CANDELINC: a general approach to multidimensional analysis of many-way arrays with linear constraints on parameters*, Psychometrika, 45 (1980), pp. 3–24.

- [9] M. CHEN AND D. KRESSNER, *Recursive blocked algorithms for linear systems with Kronecker product structure*, Numer. Algorithms, 84 (2020), pp. 1199–1216.
- [10] Z. CHEN AND L. LU, *A projection method and Kronecker product preconditioner for solving Sylvester tensor equations*, Sci. China Math., 55 (2012), pp. 1281–1292.
- [11] A. CHERTKOV AND I. OSELEDETS, *Solution of the Fokker–Planck equation by cross approximation method in the tensor train format*, Frontiers in Artificial Intelligence, 4 (2021).
- [12] A. COHEN, R. DEVORE, AND C. SCHWAB, *Analytic regularity and polynomial approximation of parametric and stochastic elliptic PDE’s*, Anal. Appl. (Singap.), 9 (2011), pp. 11–47.
- [13] A. DEKTOR, A. RODGERS, AND D. VENTURI, *Rank-adaptive tensor methods for high-dimensional nonlinear PDEs*, J. Sci. Comput., 88:36 (2021).
- [14] A. DEKTOR AND D. VENTURI, *Dynamically orthogonal tensor methods for high-dimensional nonlinear PDEs*, J. Comput. Phys., 404 (2020), p. 103501.
- [15] S. DOLGOV, D. KRESSNER, AND C. STRÖSSNER, *Functional Tucker approximation using Chebyshev interpolation*, SIAM J. Sci. Comput., 43 (2021), pp. A2190–A2210.
- [16] T. A. DRISCOLL, F. BORNEMANN, AND L. N. TREFETHEN, *The chebop system for automatic solution of differential equations*, BIT, 48 (2008), pp. 701–723.
- [17] T. A. DRISCOLL AND N. HALE, *Rectangular spectral collocation*, IMA J. Numer. Anal., 36 (2016), pp. 108–132.
- [18] T. A. DRISCOLL, N. HALE, AND L. N. TREFETHEN, *Chebfun guide*, Pafnuty Publications, Oxford, 2014.
- [19] D. EBLING, M. JAEGLE, M. BARTEL, A. JACQUOT, AND H. BÖTTNER, *Multiphysics simulation of thermoelectric systems for comparison with experimental device performance.*, J. Electron. Mater., 38 (2009), pp. 1456–1461.
- [20] B. FORNBERG, *A practical guide to pseudospectral methods*, vol. 1 of Cambridge Monographs on Applied and Computational Mathematics, Cambridge University Press, Cambridge, 1996.
- [21] D. FORTUNATO, N. HALE, AND A. TOWNSEND, *The ultraspherical spectral element method*, J. Comput. Phys., 436 (2021), p. 110087.
- [22] D. FORTUNATO AND A. TOWNSEND, *Fast Poisson solvers for spectral methods*, IMA J. Numer. Anal., 40 (2020), pp. 1994–2018.
- [23] S. GARREIS AND M. ULBRICH, *Constrained optimization with low-rank tensors and applications to parametric problems with PDEs*, SIAM J. Sci. Comput., 39 (2017), pp. A25–A54.
- [24] G. H. GOLUB AND C. F. VAN LOAN, *Matrix computations*, Johns Hopkins Studies in the Mathematical Sciences, Johns Hopkins University Press, Baltimore, MD, fourth ed., 2013.
- [25] A. GORODETSKY, S. KARAMAN, AND Y. MARZOUK, *A continuous analogue of the tensor-train decomposition*, Comput. Methods Appl. Mech. Eng., 347 (2019), pp. 59 – 84.
- [26] D. GOTTLIEB AND S. A. ORSZAG, *Numerical analysis of spectral methods: theory and applications*, Society for Industrial and Applied Mathematics, Philadelphia, Pa., 1977.
- [27] W. HACKBUSCH, *Tensor spaces and numerical tensor calculus*, vol. 42 of Springer Series in Computational Mathematics, Springer, Heidelberg, 2012.

- [28] S. HAO AND P.-G. MARTINSSON, *A direct solver for elliptic PDEs in three dimensions based on hierarchical merging of Poincaré-Steklov operators*, J. Comput. Appl. Math., 308 (2016), pp. 419–434.
- [29] B. HASHEMI AND Y. NAKATSUKASA, *Least-squares spectral methods for ODE eigenvalue problems*, arXiv e-prints, (2021), p. arXiv:2109.05384.
- [30] B. HASHEMI AND L. N. TREFETHEN, *Chebfun in three dimensions*, SIAM J. Sci. Comput., 39 (2017), pp. C341–C363.
- [31] J. S. HESTHAVEN, S. GOTTLIEB, AND D. GOTTLIEB, *Spectral methods for time-dependent problems*, vol. 21 of Cambridge Monographs on Applied and Computational Mathematics, Cambridge University Press, Cambridge, 2007.
- [32] T. HILLEN AND K. J. PAINTER, *A user’s guide to PDE models for chemotaxis*, J. Math. Biol., 58 (2009), pp. 183–217.
- [33] H. IGEL, *Wave propagation in three-dimensional spherical sections by the Chebyshev spectral method*, Geophysical Journal International, 136 (1999), pp. 559–566.
- [34] G. E. KARNIADAKIS AND S. J. SHERWIN, *Spectral/hp element methods for computational fluid dynamics*, Numerical Mathematics and Scientific Computation, Oxford University Press, New York, second ed., 2005.
- [35] O. KOCH AND C. LUBICH, *Dynamical low-rank approximation*, SIAM J. Matrix Anal. Appl., 29 (2007), pp. 434–454.
- [36] T. G. KOLDA AND B. W. BADER, *Tensor decompositions and applications*, SIAM Rev., 51 (2009), pp. 455–500.
- [37] D. KRESSNER AND C. TOBLER, *Krylov subspace methods for linear systems with tensor product structure*, SIAM J. Matrix Anal. Appl., 31 (2009), pp. 1688–1714.
- [38] ———, *Preconditioned low-rank methods for high-dimensional elliptic PDE eigenvalue problems*, Comput. Methods Appl. Math., 11 (2011), pp. 363–381.
- [39] G. LIU, A. A. QUTUB, P. VEMPATI, F. MAC GABHANN, AND A. S. POPEL, *Module-based multiscale simulation of angiogenesis in skeletal muscle*, Theor. Biol. Med. Model., 8 (2011), pp. 1–21.
- [40] G. J. LORD, C. E. POWELL, AND T. SHARDLOW, *An introduction to computational stochastic PDEs*, Cambridge Texts in Applied Mathematics, Cambridge University Press, New York, 2014.
- [41] K. MADSEN, H. NIELSEN, AND O. TINGLEFF, *Methods for Non-Linear Least Squares Problems (2nd ed.)*, DTU, 2nd ed., 2004.
- [42] J. C. MASON AND D. C. HANDSCOMB, *Chebyshev polynomials*, Chapman and Hall/CRC, 2002.
- [43] D. MCBRIDE, M. CROSS, N. CROFT, C. BENNETT, AND J. GEBHARDT, *Computational modelling of variably saturated flow in porous media with complex three-dimensional geometries*, Internat. J. Numer. Methods Fluids, 50 (2006), pp. 1085–1117.
- [44] E. A. MURAVLEVA AND I. V. OSELEDETS, *Approximate solution of linear systems with Laplace-like operators via cross approximation in the frequency domain*, Comput. Methods Appl. Math., 19 (2019), pp. 137–145.
- [45] S. OLVER, R. M. SLEVINSKY, AND A. TOWNSEND, *Fast algorithms using orthogonal polynomials*, Acta Numer., 29 (2020), pp. 573–699.

- [46] S. OLVER AND A. TOWNSEND, *A fast and well-conditioned spectral method*, SIAM Rev., 55 (2013), pp. 462–489.
- [47] S. OLVER, A. TOWNSEND, AND G. VASIL, *A sparse spectral method on triangles*, SIAM J. Sci. Comput., 41 (2019), pp. A3728–A3756.
- [48] H. P. PFEIFFER, L. E. KIDDER, M. A. SCHEEL, AND S. A. TEUKOLSKY, *A multidomain spectral method for solving elliptic equations*, Comput. Phys. Comm., 152 (2003), pp. 253–273.
- [49] R.-E. PLESSIX, *A Helmholtz iterative solver for 3D seismic-imaging problems*, Geophysics, 72 (2007), pp. SM185–SM194.
- [50] A. POPOV AND N. Y. ZHU, *Modeling radio wave propagation in tunnels with a vectorial parabolic equation*, IEEE Trans. Antennas Propag., 48 (2000), pp. 1403–1412.
- [51] N. SCHWENCK, B. FLEMISCH, R. HELMIG, AND B. I. WOHLMUTH, *Dimensionally reduced flow models in fractured porous media: crossings and boundaries*, Comput. Geosci., 19 (2015), pp. 1219–1230.
- [52] T. SHI AND A. TOWNSEND, *On the compressibility of tensors*, SIAM J. Matrix Anal. Appl., 42 (2021), pp. 275–298.
- [53] M. B. SOLEY, P. BERGOLD, A. GORODETSKY, AND V. S. BATISTA, *Functional Tensor-Train Chebyshev method for multidimensional quantum dynamics simulations*, arXiv e-prints, (2021), p. arXiv:2109.08985.
- [54] K. R. SWANSON, C. BRIDGE, J. MURRAY, AND E. C. ALVORD, *Virtual and real brain tumors: using mathematical modeling to quantify glioma growth and invasion*, Journal of the Neurological Sciences, 216 (2003), pp. 1–10.
- [55] R. A. TODOR AND C. SCHWAB, *Convergence rates for sparse chaos approximations of elliptic problems with stochastic coefficients*, IMA J. Numer. Anal., 27 (2007), pp. 232–261.
- [56] A. TOWNSEND, *Computing with functions in two dimensions*, ProQuest LLC, Ann Arbor, MI, 2014.
- [57] A. TOWNSEND AND S. OLVER, *The automatic solution of partial differential equations using a global spectral method*, J. Comput. Phys., 299 (2015), pp. 106–123.
- [58] A. TOWNSEND, H. WILBER, AND G. B. WRIGHT, *Computing with functions in spherical and polar geometries I. The sphere*, SIAM J. Sci. Comput., 38 (2016), pp. C403–C425.
- [59] L. N. TREFETHEN, *Spectral methods in MATLAB*, vol. 10 of Software, Environments, and Tools, Society for Industrial and Applied Mathematics (SIAM), Philadelphia, PA, 2000.
- [60] ———, *Approximation theory and approximation practice*, Society for Industrial and Applied Mathematics (SIAM), Philadelphia, PA, 2013.
- [61] E. ULLMANN, H. C. ELMAN, AND O. G. ERNST, *Efficient iterative solvers for stochastic Galerkin discretizations of log-transformed random diffusion problems*, SIAM J. Sci. Comput., 34 (2012), pp. A659–A682.
- [62] T. VON PETERSDORFF AND C. SCHWAB, *Numerical solution of parabolic equations in high dimensions*, M2AN Math. Model. Numer. Anal., 38 (2004), pp. 93–127.
- [63] Z. WANG AND S. F. WU, *Helmholtz equation–least-squares method for reconstructing the acoustic pressure field*, J. Acoust. Soc. Am., 102 (1997), pp. 2020–2032.
- [64] H. WILBER, A. TOWNSEND, AND G. B. WRIGHT, *Computing with functions in spherical and polar geometries II. The disk*, SIAM J. Sci. Comput., 39 (2017), pp. C238–C262.

- [65] H. XIANG AND L. GRIGORI, *Kronecker product approximation preconditioners for convection-diffusion model problems*, Numer. Linear Algebra Appl., 17 (2010), pp. 691–712.
- [66] H. XU, C. D. CANTWELL, C. MONTESERIN, C. ESKILSSON, A. P. ENGSIG-KARUP, AND S. J. SHERWIN, *Spectral/hp element methods: Recent developments, applications, and perspectives*, Journal of Hydrodynamics, 30 (2018), pp. 1–22.
- [67] S. ZHAO AND M. J. YEDLIN, *A new iterative Chebyshev spectral method for solving the elliptic equation $\nabla \cdot (\sigma \nabla u) = f$* , J. Comput. Phys., 113 (1994), pp. 215–223.
- [68] M. S. ZHDANOV, S. K. LEE, AND K. YOSHIOKA, *Integral equation method for 3D modeling of electromagnetic fields in complex structures with inhomogeneous background conductivity*, Geophysics, 71 (2006), pp. G333–G345.